Journal of the European Ceramic Society 21 (2001) 1905–1908

www.elsevier.com/locate/jeurceramsoc

Microstructures and properties of semi-conductive $Pb_{0.6}Sr_{0.4}TiO_3$ ceramics using $PbTiO_3$-coated $SrTiO_3$ powders

Ping-Hong Chen [a], Han-Chang Pan [a], Chen-Chia Chou [a,*], I.-Nan Lin [b]

[a] *Department of Mechanical Engineering, National Taiwan University of Science and Technology, 43 Keelung Road Sec.4, Taipei 106, Taiwan*
[b] *Materials Science Center, National Tsing-Hwa University, Hsinchu 300, Taiwan*

Received 4 September 2000; received in revised form 17 November 2000; accepted 25 November 2000

Abstract

Microstructures and properties of semi-conductive $Pb_{0.6}Sr_{0.4}TiO_3$ ceramics fabricated from $PbTiO_3$-coated $SrTiO_3$ powders were investigated using X-ray and electron diffraction, transmission electron microscopy and energy dispersive spectroscopy. $PbTiO_3$-coated $SrTiO_3$ powders were prepared for simulating the core-shell structure in $Pb_{0.6}Sr_{0.4}TiO_3$ ceramics, which were sintered by microwave, rapid thermal and conventional sintering processes. After TEM investigations and EDS analyses, it is found that the microwave-sintered specimens preserve the starting core-shell structure more effectively than the conventional and rapid thermal sintered specimens. According to our core-shell model, the microwave-sintered specimens show single T_c and the conventional, rapid thermal sintered specimens exhibit double T_c behavior, as verified by the resistivity–temperature ($\rho-T$) properties. Our interpretation implies that the core-shell structure may be the primary factor affecting the $\rho-T$ properties. © 2001 Elsevier Science Ltd. All rights reserved.

Keywords: Electron microscopy; Ferroelectric properties; Microwave processing; Perovskites; PTC devices

1. Introduction

The positive temperature coefficient of resistivity (PTCR) of semiconducting ceramics with $(Sr,Ba)TiO_3$, $(Pb,Sr)TiO_3$ or $(Pb,Ba)TiO_3$ compositions, possessing the Curie temperature in the range −30–360°C,[1–4] have been thoroughly developed. Conventionally, these PTCR materials are prepared by the mixed oxide method and sintered in a resistance-furnace. A high sintering temperature (1260–1350°C) and long soaking period (0.5–11 h) are required to densify the materials. Close control of the sintering atmosphere is required to prevent the loss of Pb-species in Pb-containing materials even when the liquid phase sintering aids are applied.[5]

The microwave sintering process, on the other hand, has been observed to densify the ceramic materials at a very rapid rate and at a substantially lower temperature.[6–8] Some intriguing properties were also observed.[9,10] However, the corresponding microstructure was seldom studied.[11] To elucidate the relationship among the process, properties and microstructures of the materials, specimens prepared by $PbTiO_3$-coated $SrTiO_3$ powders are sintered by various sintering processes and then the corresponding microstructures are investigated by electron microscopy and EDS. $\rho-T$ properties were also interpreted based upon the observed microstructure in the present work.

2. Experimental

$PbTiO_3$-coated $SrTiO_3$ powders were prepared by a sol–gel method in order to simulate a core-shell structure.[12] Solutions containing Ti^{4+} and Pb^{2+} were prepared by mixing titanium isopropoxide, 2-methoxyl ethanol and acetyl acetone, as well as lead acetate trihydrate and 2-methoxyl ethanol. $PbTiO_3$ sol–gel was then coated on oxide-made $SrTiO_3 + 1Y3T5S$ (where $Y{:}Y_2O_3$, $T{:}TiO_2$, S: SiO_2) by mixing the solutions and the powders. After solvent evaporation, powders were obtained by heating at 200°C — 4 h, 500°C — 4 h and then calcined at 800°C for 2 h. The nominal composition of the powders was $0.6PbTiO_3 + 0.4(SrTiO_3 + 1Y3T5S) + 1Y5S$. The green compacts made of these powders were sintered by microwave (MS), rapid thermal (RTS), or conventional furnace (CS) sintering processes.[10–12]

---

* Corresponding author. Tel.: +886-2-2737-6493; fax: +886-2-2737-6460.
E-mail address: ccchou@mail.ntust.edu.tw (C.-C. Chou).

PII: S0955-2219(01)00140-6

Resistivity–temperature ($\rho-T$) properties of these samples were measured using a HP3457A multimeter after the In–Ga alloy was rubbed onto the sample surface to serve as electrodes. The microstructure of the sintered samples was examined using a Jeol JSM-840A scanning electron microscope (SEM) and a Jeol JXA8800M electron probe microanalyser (EPMA). Jeol 2000FXII scanning transmission electron microscope (STEM) with energy dispersive spectroscope (EDS) system was also employed for the investigations of the internal structures of specimens.

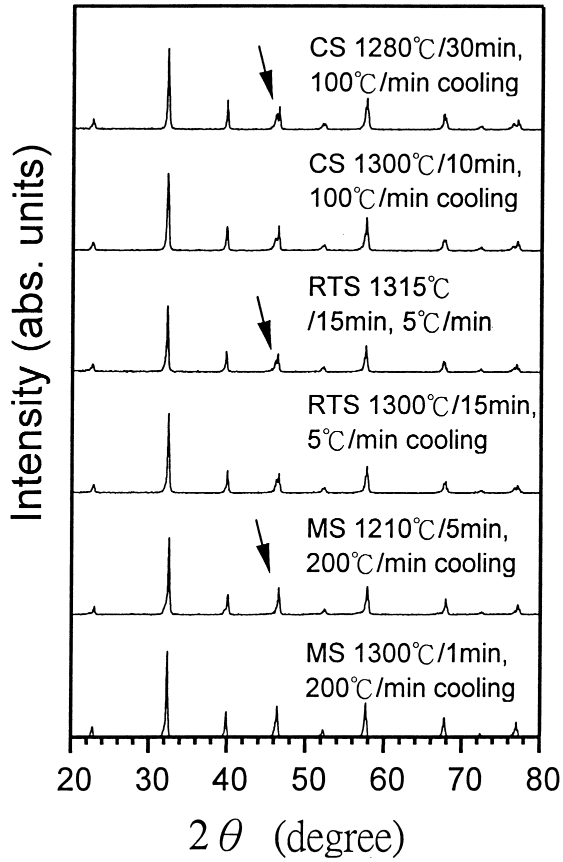

Fig. 1. X-ray diffraction patterns of $PbTiO_3$-coated $SrTiO_3$ specimens sintered by microwave, rapid thermal and conventional sintering processes.

3. Results and discussion

Fig. 1 shows that the X-ray diffraction patterns of $PbTiO_3$-coated $SrTiO_3$ specimens sintered at various sintering conditions exhibit different average tetragonality. The results indicate that CS-specimens are tetragonal with high c/a ratio, MS-specimens are nearly cubic and RTS-specimens possess medium tetragonality.

Fig. 2(a) is a TEM micrograph which shows the internal structure of a microwave-sintered $PbTiO_3$-coated $SrTiO_3$ specimen. In addition to that the grains exhibit very few or no domain boundaries, domain boundaries in grains are easily affected by the electron beam, consistent with the X-ray diffraction results.

On the other hand, the domain arrangements of RTS- and CS-specimens are quite different from those of MS-specimens. In CS-specimens (CS 1300°C/10 min, 100°C/min cooling), different variants of domain boundaries intersect in the grain interior and therefore the complicated domain arrangements appear, as shown in Fig. 2(b). RTS-specimens (RTS1300°C/15 min, 5°C/min cooling) possessing less complicated domain arrangements can be seen in Fig. 2(c). The reason why the $PbTiO_3$-coated $SrTiO_3$ specimens of different sintering process show this large difference in domain arrangements can be attributed to the tetragonality of the materials. In general, the formation of complicated domain arrangements implies that a large strain field is induced during the phase transformation of paraelectric to ferroelectric state. To release high internal stress, many sets of domains form in a grain and, therefore, we see complicated domain configurations in specimens, and vice versa.

To understand the detailed arrangements of the core-shell structures of this kind[11–13] and their effects on $\rho-T$ properties, the core-shell structures are further

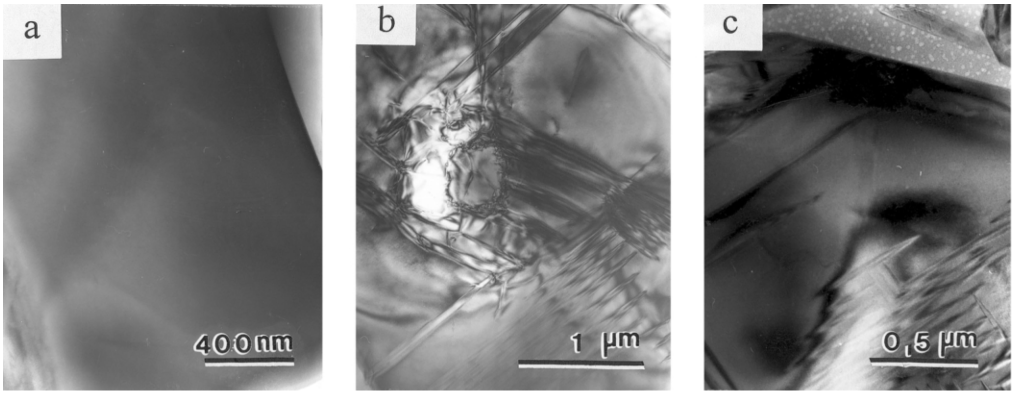

Fig. 2. TEM micrographs showing domain arrangements of (a) MS (1150/10 min); (b) CS (1300/10 min, 100°C/min cooling); (c) RTS (1300°C/15 min, 5°C/min cooling) $PbTiO_3$-coated $SrTiO_3$ specimens.

investigated. Fig. 3 shows the core-shell structure and the corresponding EDS analysis of a MS-specimen. The EDS results show that a portion of Pb diffuse into the grain interior, and some stay in the liquid-phase-sintering area because of the eutectic reaction of $PbTiO_3$ with SiO_2. At the shell region, the original $PbTiO_3$ composition had changed to $Pb_xSr_{1-x}TiO_3$ owing to the element interdiffusion between the core and the shell regions.

The heating and sintering time of the conventional furnace sintering process are longer than that of the microwave-sintering process, and hence the core-shell interdiffusion in CS-specimens must be very serious. In the TEM investigations, we find that the core-shell structure was not always observed in many grains of CS-specimens. If any, the amount is relatively small. Fig. 4 shows a grain possessing a core-shell structure and the corresponding EDS analysis of a CS-specimen. The EDS results indicate that interdiffusion between the elements of the $SrTiO_3$ core and the $PbTiO_3$ shell regions is serious and a thin shell without high Pb-content is observed.

Based upon a core-shell model,[10,11] we predict that the $\rho-T$ curves of every specimens will not present single T_c at the temperature of 490°C because the shell regions were not pure $PbTiO_3$ in the specimens. Fig. 5 shows the $\rho-T$ curves of $PbTiO_3$-coated $SrTiO_3$ specimens sintered by different sintering processes. Predictably, all the specimens do not show a single T_c at the temperature of 490°C. Nevertheless, the MS-specimen (MS 1210°C/5 min, 200°C/min cooling) show a single T_c at about 420°C (T_{cs}). According to the core-shell model, this single T_c behavior is caused by the low resistance electron conduction path (shell region) when the temperature between T_{cc} and T_{cs}. In our investigations, the MS-specimen has the widest shell thickness (0.45 μm) and the highest Pb-content (35%) at the shell regions. When the temperature is in-between T_{cc} and T_{cs}, the Schottky barriers at core-to-shell boundaries and grain boundaries are, therefore, suppressed by the spontaneous polarization charges in the shell regions, resulting

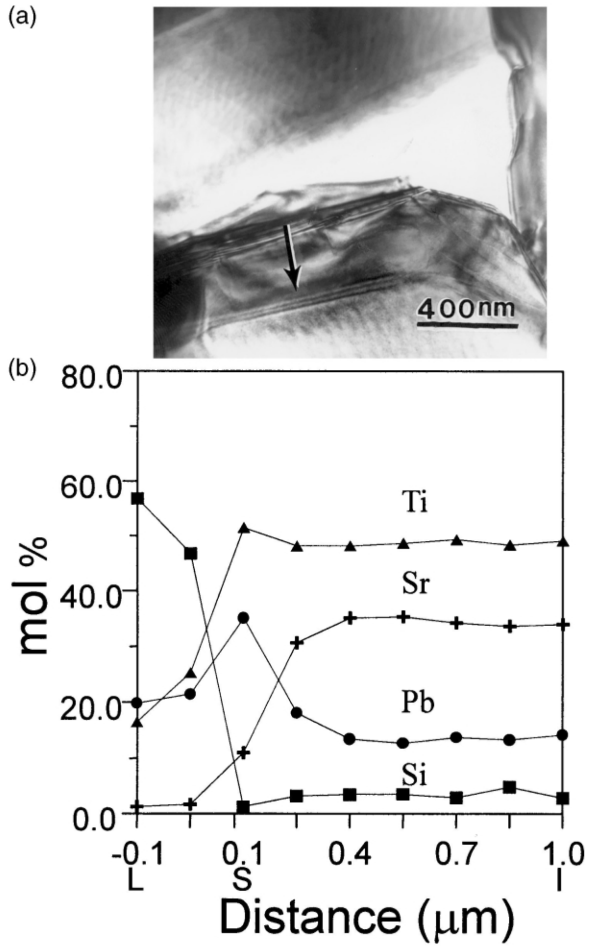

Fig. 3. (a) TEM micrograph showing the core-shell structure and (b) the corresponding EDS analysis of microwave sintered $PbTiO_3$-coated $SrTiO_3$ specimen (MS 1210°C/5 min, 200°C/min cooling) (L: liquid phase sintering area; S: shell region; I: grain interior).

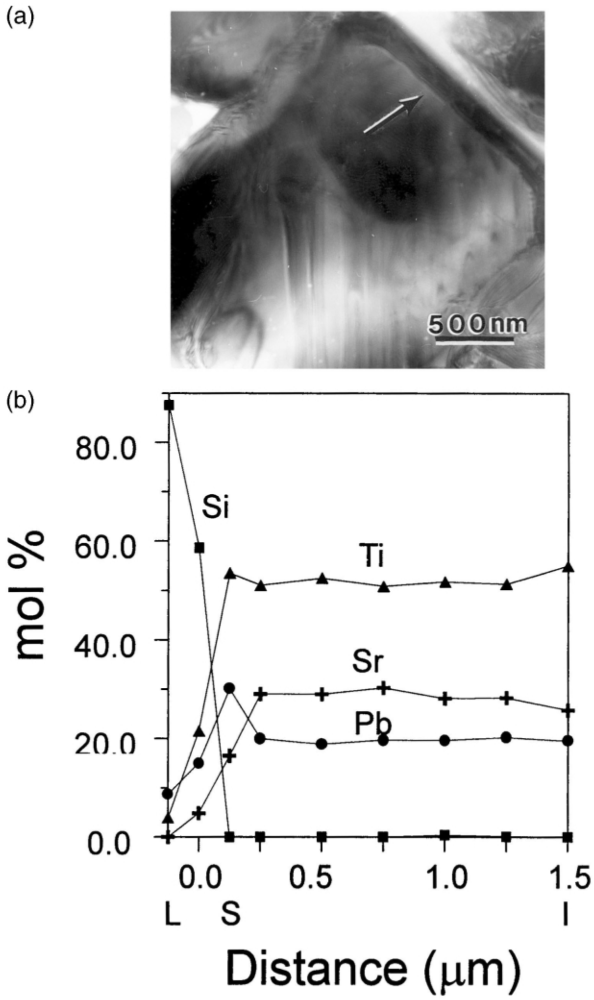

Fig. 4. (a) TEM micrograph showing the core-shell structure and (b) the corresponding EDS analysis of conventional furnace sintered $PbTiO_3$-coated $SrTiO_3$ specimen (CS 1300°C/10 min, 100°C/min cooling) (L: liquid phase sintering area; S: shell region; I: grain interior).

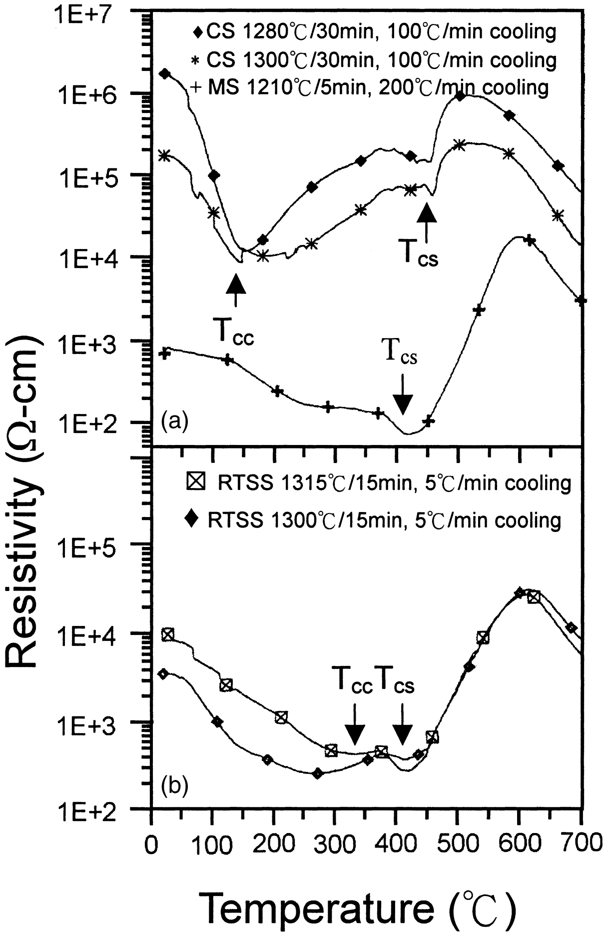

Fig. 5. Resistivity–temperature curves of the PbTiO$_3$-coated SrTiO$_3$ specimen prepared by (a) conventional and microwave sintering, and (b) rapid thermal sintering.

in a low resistance electron conduction path at the shell regions. A single T_c behavior was then observed in the $\rho - T$ curve of a MS-specimen.

On the other hand, the starting core-shell structure of CS-specimens could not preserve original compositions, and leads to an abrupt increase of resistivity at the temperature between T_{cc} and T_{cs}. When the temperature reaches T_{cs}, the Schottky barriers at core-to-shell boundaries and grain boundaries rise again and then another T_c forms at T_{cs}. The double T_c behavior was therefore observed in the $\rho - T$ curve of CS-specimen. In RTS specimens, although the core-shell structure can be preserved, the Pb-content of the shell region is relatively lower comparing with MS-specimens. Hence, the $\rho - T$ curve shows an unclear double T_c behavior, as seen in Fig. 5(b).

Above interpretations not only explain the relationship between the core-shell structures of PbTiO$_3$-coated SrTiO$_3$ specimens, prepared by different sintering processes, and their corresponding $\rho - T$ curves, but also verify that the core-shell structures critically affect $\rho - T$ properties.

4. Conclusions

PbTiO$_3$-coated SrTiO$_3$ powders were prepared for simulating the core-shell structure in Pb$_{0.6}$Sr$_{0.4}$TiO$_3$ ceramics, which were fabricated by microwave, rapid thermal and conventional sintering processes. After TEM investigations and EDS analyses, it is found that the microwave-sintered specimens preserve the starting core-shell structure more effectively than the conventional and rapid thermal sintered specimens. According to our core-shell model, the microwave-sintered specimens show single T_c and the conventional, rapid thermal sintered specimens exhibit double T_c behavior, as verified by the $\rho - T$ properties. Our results imply that the core-shell structure may be the primary factor affecting the $\rho - T$ properties.

References

1. Wakino, K. and Fujikawa, N., *Electron. Ceram.*, 1971, **2**, 65.
2. Kuwabara, M., Lead titanate ceramics with positive temperature coefficient of resistivity. *J. Am. Ceram. Soc.*, 1990, **73**, 1438–1439.
3. Hamata, Y., Takuchi, H. and Zomara, K., V-shaped PTCR materials, Japan. Patent 63-280401, 17 November 1988.
4. Lee, C. K., Lin, I. N. and Hu, C. T., Evolution of microstructure and V-shaped positive temperature coefficient of resistivity of (Pb$_{0.6}$Sr$_{0.4}$)TiO$_3$ materials. *J. Am. Ceram. Soc.*, 1994, **77**, 1340–1344.
5. Cheng, H. F., Lin, T. F., Hu, C. T. and Lin, I. N., Effect of sintering aids on microstructures and PTCR characteristics of (Sr$_{0.2}$Ba$_{0.8}$)TiO$_3$ ceramics. *J. Am. Ceram Soc.*, 1993, **76**, 827–832.
6. Sutton, W. H., Microwave processing of ceramic materials. *Am. Ceram. Soc. Bull.*, 1989, **68**, 376.
7. Warrier, K. G. K., Varma, H. K., Mani, T. V. and Damodaran, A. D., Rapid method for the preparation on 123 superconductor using microwaves. *J. Am. Ceram. Soc.*, 1992, **75**, 1990–1992.
8. Janney, M. A., Calhoun, C. L. and Kimrey, H. D., Microwave sintering of solid oxide fuel cell materials: I, Zirconia–8 mol% Yttria. *J. Am. Ceram. Soc.*, 1992, **75**, 341–346.
9. Chang, H. Y., Liu, K. S., Chen, H. W., Hu, C. T., Lin, I. N., Shaw, B. J. and Tan, J. T., V-shape positive temperature coefficient of resistivity characteristics of microwave-sintered (Sr$_{0.4}$Pb$_{0.6}$)TiO$_3$. *Mater. Chem. Phys.*, 1995, **42**, 258–263.
10. Chang, H. Y., Liu, K. S., Hu, C. T., Lin, T. F. and Lin, I. N., Double critical temperature characteristics of semiconducting (Ba$_{0.7}$Pb$_{0.3}$)TiO$_3$ materials prepared by microwave sintering. *J. Appl. Phys.*, 1996, **80**, 4553–4559.
11. Chou, C. C., Chang, H. Y., Lin, I. N., Shaw, B. J. and Tan, J. T., Microscopic examination of the microwave sintered (Pb$_{0.6}$Sr$_{0.4}$) TiO$_3$ positive-temperature-coefficient resistor materials. *Jpn. J. Appl. Phys.*, 1998, **37**, 5269–5272.
12. Lin, Y. Y., *High Temperature (Pb,Sr)TiO$_3$ PTCR Materials.* Master thesis, Tsing-Hua University, Taiwan, 1996.
13. Uchikoba, F. and Sawamura, K., Core-shell domain structure in lead complex perovskite material. *Jpn. J. Appl. Phys.*, 1993, **32**, 4258–4260.